Available online at www.sciencedirect.com
SCIENCE DIRECT®
PERGAMON
Scripta Materialia 48 (2003) 1117–1122
Scripta MATERIALIA
www.actamat-journals.com

Comparison of grain boundary sliding in fine grained Mg and Al alloys during superplastic deformation

Y.N. Wang, J.C. Huang *

Institute of Materials Science and Engineering, National Sun Yat-Sen University, Kaohsiung 804, Taiwan, ROC

Received 31 October 2002; received in revised form 27 November 2002; accepted 5 December 2002

Abstract

The surface topography resulting from grain boundary sliding (GBS) in warm-extruded AZ61 sheets was investigated after tensile superplastic loading, and compared with previous examinations on Al base alloys. GBS was observed to prevail from the very initial stage; ~60% of total strain was contributed by GBS due to the high fraction (88%) of high angle boundaries in AZ61, distinctly different from the case of Al alloys.

Keywords: Mg alloys; Superplasticity; Grain boundary sliding; Electron backscattering diffraction; Extrusion

1. Introduction

The major mechanisms involved in superplastic deformation include grain boundary sliding (GBS), grain rotation, grain boundary migration (GBM), and accommodation processes such as diffusion creep and transgranular dislocation motion. Amongst these mechanisms, GBS is the dominant mechanism based on the large amount of experimental data. The activation energy may be close to that of lattice diffusion or grain boundary diffusion.

Magnesium alloys have high potential as lightweight structure materials owing to their low density. Recently, great attention has been attracted on the superplasticity and superplastic forming of Mg based alloys [1–10]. These experimental data indicated that GBS still appears to be the dominant deformation process, including those that exhibit low temperature superplasticity and/or high strain rate superplasticity [3,4,7,10]. With the detailed examinations completed on the GBS behaviors in fine-grained Al alloys, very limited studies were done on the Mg counterparts.

Direct observations of GBS in some Al or Ti alloys [11–13] have shown that cooperative grain boundary sliding (CGBS), occurring through the movement of grain groups as an entity, would initiate from the beginning stage of superplastic deformation. And cooperative grain boundary migration (CGBM) may also play a cooperative role [14]. Individual GBS would typically occur at later stages.

The aim of the current study is emphasized on surface topographic characterization of superplastic tensile-loaded AZ61 Mg alloy; and the results are compared with our previous study on the

* Corresponding author. Tel.: +886-7-525-2000/4070x4063; fax: +886-7-525-4099.
E-mail address: jacobc@mail.nsysu.edu.tw (J.C. Huang).

1359-6462/03/$ - see front matter © 2003 Acta Materialia Inc. Published by Elsevier Science Ltd. All rights reserved.
doi:10.1016/S1359-6462(02)00615-2

Al base alloys. The origins of the grain boundary step, striated bands (SB), cavities, and fibers on the specimen surface are examined. Topographic evolutions resulting from different strain levels and the contribution of GBS to overall strain are of major concern. The possible reasoning for GBS in the current material is also discussed.

2. Experiential procedure

The material used is a commercial AZ61 alloy (Mg–5.88wt.%Al–0.74wt.%Zn). One-step extrusion process was undertaken using an extrusion ratio of 40:1 at ~300 °C and a strain rate of $\sim 10^{-2}$ s^{-1}, resulting in a sheet of 100 mm in width and 2 mm in thickness. The microstructure of coarse equiaxed colonies of α-Mg phase in the as-cast AZ61 alloy (~80 μm) has been changed into a structure of considerably refined grains with an average line intercept size of ~6 μm, which implied that extensive dynamic recrystallization has taken place during warm extrusion process. This is quite different from the ill-defined subgrain and partially recrystallized microstructures observed in the thermomechanically processed 8090 Al–Li–Cu–Mg [12,15] or 5083 Al–Mg–Mn [16] alloys.

The tensile axis is normal to the extruded direction, with a gauge length of 10 mm and width of 3 mm. Constant crosshead speed tensile tests were conducted on an Instron 5583 universal testing machine equipped with a three-zone furnace at temperature ranging from 573 to 673 K and initial strain rate range from 1×10^{-4} to 1×10^{-2} s^{-1}. In order to examine the operation of GBS, tensile tests to different strain levels, e.g., $\varepsilon = 0.10$ (10%), 0.44 (55%), 1.1 (200%) and 1.78 (500%-fractured) were performed at 623 K and 1×10^{-3} s^{-1}. Marker lines parallel to the loading direction were made on the polished specimen surface prior to tensile loading. The surface morphology of tested samples was examined by a Jeol 6335 field emission scanning electron microscopy (FEG-SEM). The misorientation angle distribution of the as-worked alloys was examined using electron back-scattered diffraction (EBSD) attached with the FEG-SEM.

3. Results and discussion

3.1. Basic deformation characteristics

The experimental results illustrate that the superplastic deformation at 573–673 K was uniform and with the highest elongation to failure of 920% occurred at 623 K and 1×10^{-4} s^{-1}, as shown in Fig. 1.

The flow stress against strain rate (σ–$\dot{\varepsilon}$) curves at 573–673 K determined by strain rate step tests are plotted in Fig. 2(a). The mean apparent strain rate sensitivity exponent (m_a value) of 0.45 was obtained from the slope of the curves over the tested strain rates, suggesting that GBS might be a dominant deformation process [17]. The apparent activation energy Q_a can be evaluated according to the equation

$$Q_a = -R \left. \frac{\partial(\ln \dot{\varepsilon})}{\partial(1/T)} \right|_{\sigma=\text{constant}}, \quad (1)$$

where R and T are gas constant and absolute temperature, respectively. Taking $\sigma = 20$ MPa, Q_a was estimated from the slope of the plot of $\ln \dot{\varepsilon}$ against $1000/RT$ based on Eq. (1) (Fig. 2(b)). The apparent activation energy over 573–673 K is 132 ± 2 kJ/mol, which is close to that for lattice diffusion of magnesium (135 kJ/mol) [18]. Based on the calculated data of m_a and Q_a, it is suggested that the dominant deformation mechanism in the present alloy is GBS accommodated by slip, the

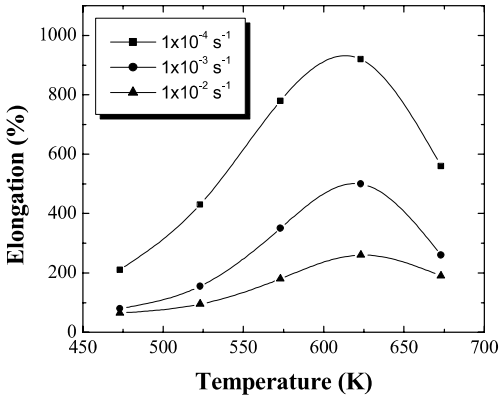

Fig. 1. Tensile elongations of the AZ61 specimens as a function of test temperatures and strain rate.

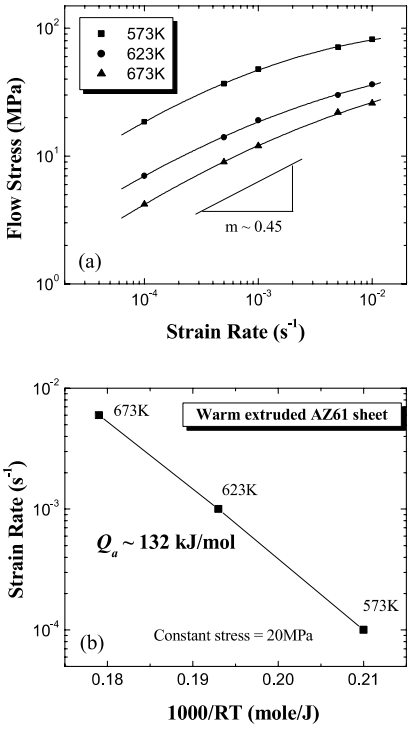

Fig. 2. The analyses on the superplastic AZ61 alloy for extraction of (a) apparent strain rate sensitivity m_a, (b) apparent activation energy Q_a.

latter is in-turn controlled by lattice diffusion over 573–673 K.

3.2. SEM observations

Fig. 3 shows the SEM surface morphology of strained specimens at various strain levels of 0.10, 0.44, 1.10 and 1.78 (fractured) loading at 623 K and 1×10^{-3} s^{-1}.

In the initial stage of superplastic deformation as the strain reached ~0.1 (10%), GBS can be easily seen from the clear offsets of pre-scratched marked lines and, especially, from the large number of grain boundary steps as shown in Fig. 3(a). Formation of SB and fibers was not significant in this region. It should be noted that almost all surface grains in the AZ61 alloy have been involved in GBS operation, namely, individual GBS rather than CGBS was undertaken from the very beginning stage of superplastic straining. This is distinctly different from the case usually observed in aluminum alloys [11–13]. In the thermomechanically processed or similarly extruded fine grained 8090 or 5083 Al alloys tensile-strained to $\varepsilon \sim 0.1$–0.5 at 473–673 K, the occurrence frequency of GBS or CGBS was low; dislocation activity and dynamic recrystallization were heavily operative over this initial stage.

As the strain reached ~0.44 (55%) in the AZ61 specimen, GBS offsets at individual grains were progressively further developed as shown in Fig. 3(b). Formation of SB was more pronounced and the SB height also increased in this deformation stage. The SB is a result of the newly exposed face of the grain, which inclines to the specimen surface, resulting from grain sliding upward and downward relative to specimen surface. Formation of some cavities by GBS was also found, and these cavities were usually nucleated at triple junction points as well as grain boundaries. Fibers were still rarely found at this stage. The grain shape still remained essentially equiaxed after deformation to $\varepsilon \sim 0.44$, implying that intragranular dislocation movements occurred only as accommodation to facilitate GBS.

When the total strain reached ~1.1 (200%), some fibers were observed in this stage as shown in Fig. 3(c), usually accompanied with cavity growth and the separation of grains. The direction of fibers seems to be basically parallel to tensile axis. The formation of fibers has been discussed previously in the literature [19,20]. More cavities were observed in the AZ61 specimen strained to 200%.

When the total strain reached ~1.78 (fractured), much more fibers between adjacent grains along tensile direction and wide striations on surface grains were clearly observed in this deformation stage as shown in Fig. 3(d). The wide striation on surface grains provides evidence of new fresh grains emerging from the interior of the specimen by GBS. The present experimental results showed that fibers always formed at grain boundary with elongated cavities, and grain separation was the origin of fiber formation. It appears that grain separation also played a minor role in contributing to the total strain in addition to GBS.

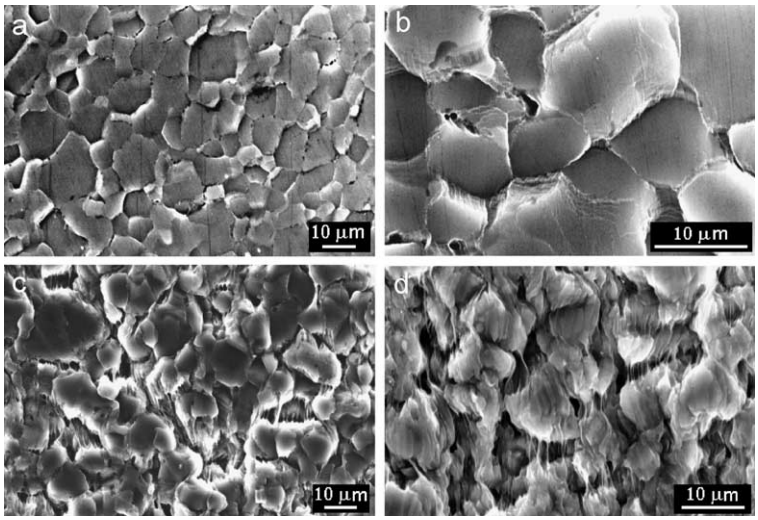

Fig. 3. SEM micrographs of the AZ61 specimens loaded at 623 K and 1×10^{-3} s^{-1}, showing the typical topography formed at different strain levels: (a) 0.1 (10%), (b) 0.44 (55%), (c) 1.1 (200%), and (d) 1.78 (500%). The tensile axis is along the vertical direction.

3.3. Strain contributed by GBS

The strain contributed by GBS (ε_{GBS}) to the total strain (ε_{Total}) can be calculated by the following expression [21],

$$\varepsilon_{GBS} = \phi \bar{w}/\overline{L}, \tag{2}$$

and

$$R_{GBS} = \varepsilon_{GBS}/\varepsilon_{Total}, \tag{3}$$

where ϕ is a geometrical constant which taken as 1.5 [21], and $\overline{L}$ is the mean linear intercept grain size, $\bar{w}$ is the main transverse offsets along a longitudinal marker lines, and R_{GBS} is the contribution of GBS. Estimation from the marker line offsets gives the GBS contribution to be around 55% and 60% at strain of 0.10 and 0.44, respectively, as illustrated in Table 1.

Table 1
Estimation of strain contribution from GBS (R_{GBS}) at strains of 0.10 and 0.44 in the warm extruded AZ61 sheet

True strain	0.10	0.44
Elongation (%)	10	55
$\bar{w}$ (μm)	0.46	2.36
$\overline{L}$ (μm)	12.6	13.4
ε_{GBS}	0.055	0.264
R_{GBS} (%)	55	60

Around 50 offsets were measured.

It should be noted that the procedure used to measure GBS, as given by Eq. (2) with a constant of 1.5, will lead to a maximum possible value of ~50–70% for the GBS contribution because of inherent difficulties in the measuring procedure [22]. In other words, the current measurements of $R_{GBS} = 55\%$ and 60% already represent nearly 90–100% of the total strain is contributed by GBS in the present AZ61 alloy.

The high R_{GBS} value of ~60% for the warm extruded AZ61 sheet in the initial tensile straining stage with $\varepsilon < 0.5$ is significantly higher than those values (around 20–30%) obtained from the Al alloy [12,16] after similar processing, as compared in Table 2. It usually needs further tensile superplastic straining to $\varepsilon \sim 1.0$ for Al base alloys before R_{GBS} can reach 60% (e.g., fully accounting for the superplastic deformation strain). The activation of individual GBS in the current Mg alloy seems to start from the onset of tensile straining. The grain boundary character in the AZ61 Mg sheet under the as-extruded condition seems to be much more favorable for GBS along most grain boundaries.

3.4. Misorientation distribution

It is well known that the grain boundary structure, or character, is related to its character-

Table 2
Comparison of the contribution from GBS in the fine grained AZ61 Mg alloy with those measured from the similarly processed 8090 Al [12] and 5083 Al [16] alloys

	T (K)	$\dot{\varepsilon}$ (s^{-1})	ε	R_{GBS} (%)
8090 Al	623	1×10^{-3}	0.50	20
	623	1×10^{-3}	1.10	48
5083 Al	523	1×10^{-3}	0.45	27
	523	1×10^{-3}	1.30	62
AZ61 Mg	623	1×10^{-3}	0.10	55
	623	1×10^{-3}	0.44	60

istic interfacial energy value, rate of mobility, and superplastic deformation rate-controlling mechanism, such as GBS [16,23,24]. It has generally been thought that random (disordered) high angle boundaries (HAB) are desirable for superplastic flow by GBS; while low energy boundaries such as low angle boundaries or coincident site lattice boundaries such as coherent twin boundaries, are nearly immobile and do not support superplastic deformation by GBS.

It has been shown experimentally that CGBS, occurring through the movement of grain group as an entity, usually occurred during the initial stage of superplastic deformation in some superplastic Al or Ti base alloys [11–13]. Furthermore, the migration of grain boundary during superplastic deformation may also exhibit a cooperative character. The boundaries that first undergo CGBS or CGBM are those with high angle and well-defined grain boundaries. For a microstructure with predominantly low angle subgrain boundaries and some CSL boundaries, as in most processed fine-grained Al alloys, individual GBS cannot operate along all boundaries during the initial superplastic straining, but only find its way to proceed along the special HAB though the CGBS mechanism. In such a case, the marker line offsets can only be observed once in may be 10 grain boundaries [12,16], and GBS would not contribute a great percentage to the total strain. It will require a minimum strain for dynamic recovery and dynamic recrystallization to render a high percentage of HAB favorable for smooth GBS.

The distributions of grain boundary misorientations measured by EBSD in the as-processed AZ61 Mg and 5083 Al alloys are shown in Fig. 4. Each angle misorientation was measured directly across a boundary; and a minimum of 500 boundaries was included for meaningful statistics. It was found that the occurrence fraction of HAB (>15°) in the warm extruded AZ61 Mg sheet (Fig. 4(a)) is as high as 88%, significantly higher than the 45–65% in the warm-worked 5083 Al (Fig. 4(b)) [16] and 2004 Al alloys [25]. This result also supports that dynamic recovery and dynamic recrystallization have undertaken thoroughly during the current warm extrusion process at ~573 K. It appears that the relatively lower fraction of HAB is the reason for superplastic flow in Al alloys to proceed by CGBS during the initial stage, and the relatively high HAB fraction is responsible for superplastic flow in the current Mg alloys carried by individual GBS during the initial superplastic stage.

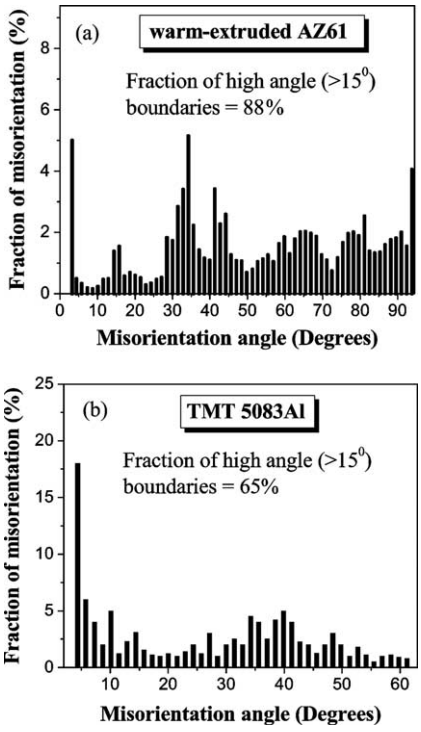

Fig. 4. Distributions of grain boundary misorientation of (a) the present warm-extruded AZ61 and (b) the thermomechanically treated 5083 alloy sheet, measured by EBSD.

The lattice and grain boundary diffusion rates of Mg at the working temperatures of 573 K are 4.7×10^{-17} m^2/s and $2 \times 10^{-20}\delta$ m^3/s, respectively, (where δ is the grain boundary width), much higher than the values of 1.8×10^{-17} m^2/s and $1.1 \times 10^{-21}\delta$ m^3/s for Al [18]. The faster diffusion rate in AZ61 results in much faster and more complete dynamic recovery and dynamic recrystallization, and in turn results in a much higher HAB fraction and the early activation of individual and effective GBS from the onset of superplastic flow.

4. Conclusion

1. Obvious individual GBS was observed during the initial stage of superplastic deformation in the warm-extruded AZ61 specimen. The R_{GBS} values was measured to be around 60%, implying that nearly all of the total strain was contributed by GBS during the early superplastic stage in AZ61. The high value of R_{GBS} is significantly higher than the case of similarly processed Al alloys under similar loading conditions.
2. SB were found to form around grain boundaries, indicating that the bands are the newly exposed faces of grains, which incline to the specimen surface, resulting from the sliding of grains upward and downward.
3. Both the size and number density of cavities increased with increasing superplastic strain. Fibers always formed at grain boundaries with elongated cavities, and grain separation was the origin of fiber formation.
4. The relatively high fraction (88%) of HAB (>15°) in the current warm-extruded AZ61 Mg sheet appears to be responsible for the efficient individual GBS operating from the initial deformation stage. This phenomenon is distinctly different from the observation in similarly worked Al alloys.
5. The cause for the different behavior of GBS operation in the initial stage of superplastic straining in Mg and Al alloys is mainly owing to the faster diffusion and dynamic recrystallization rate in the Mg base alloys.

Acknowledgements

The authors would like to gratefully acknowledge the sponsorship from National Science Council of ROC under the projects NSC 89-2216-E-110-043 and NSC 90-2216-E-110-024. The author Y.N. Wang is grateful to the post-doc sponsorship from NSC under the contrast NSC 90-2816-E-110-0001-6.

References

[1] Mabuchi M, Iwasaki H, Yanase K, Higashi K. Scripta Mater 1995;36:681.
[2] Watamabe H, Mukai T, Higashi K. Scripta Mater 1999;40:477.
[3] Mabuchi M, Ameyama K, Iwasaki H, Higashi K. Acta Mater 1999;47:2047.
[4] Watamabe H, Mukai T, Kohzu M, Tanabe S, Higashi K. Acta Mater 1999;47:3753.
[5] Mohri T, Mabuchi M, Nakamura M, Asahina T, Iwasaki H, Aizawa T, Higashi K. Mater Sci Eng A 2000;290:139.
[6] Kim WJ, Chung SW, Chung CS, Kum D. Acta Mater 2001;49:3337.
[7] Bussiba A, Artzy AB, Shtechman A, Ifergan S, Kupiec M. Mater Sci Eng A 2001;302:56.
[8] Wu X, Liu Y. Scripta Mater 2002;46:269.
[9] Tan JC, Tan MJ. Scripta Mater 2002;47:101.
[10] Watanabe H, Mukai T, Ishikawa K, Higashi K. Scripta Mater 2002;46:851.
[11] Zelin MG, Bieler TR, Mukherjee AK. Metall Mater Trans A 1993;24:1208.
[12] Pu HP, Liu PC, Huang JC. Metall Mater Trans A 1995;26:1153.
[13] Chen TR, Huang JC. Metall Mater Trans A 1999;30:53.
[14] Zelin MG, James WR, Mukherjee AK. J Mater Sci Lett 1993;24:1208.
[15] Pu HP, Huang JC. Scripta Metall Mater 1993;28:1125.
[16] Hsiao IC, Su SW, Huang JC. Metall Mater Trans A 2000;31:2169.
[17] Sherby OD, Wadsworth J. Prog Mater Sci 1989;33:169.
[18] Frost HJ, Ashby MF. In: Deformation mechanism maps. Oxford: Pergamon Press; 1982. p. 44.
[19] Novikov II, Portnoy VK, Terentieva TE. Acta Metall Mater 1981;29:1077.
[20] Rai G, Grant NJ. Metall Mater Trans A 1983;14:1451.
[21] Langdon TG. Metall Mater Trans 1972;3:797.
[22] Langdon TG. Mater Sci Eng A 1994;174:225.
[23] Watanabe T. Mater Sci Eng A 1994;176:39.
[24] McNelley TR, Mcmahon ME. Metall Mater Trans A 1996;27:2252.
[25] McNelley TR, Mcmahon ME. Metall Mater Trans A 1997;28:1879.